

A Malaria Control Model using Mobility Data: An Early Explanation of Kedougou Case in Senegal

Lynda Bouzid Khiri¹, Ibrahima Gueye³, Hubert Naacke¹, Idrissa Sarr² and Stéphane Gancarski¹

¹Sorbonne Université, Laboratoire d'Informatique de Paris 6, LIP6, F-75005, France

²Cheikh Anta Diop University, Department of Mathematics and Computer Science, Fann BP, 5005, Dakar, Senegal

³Ecole Polytechnique de Thiès, LTISI, Senegal

Keywords: Malaria Control, Mobility Model, Discrete Simulation, Data Analysis.

Abstract: Studies in malaria control cover many areas such as medicine, sociology, biology, mathematics, physics, computer science and so forth. Researches in the realm of mathematics are conducted to predict the occurrence of the disease and to support the eradication process. Basically, the modeling methodology is predominantly deterministic and based on differential equations which take into account important clinical and biological features. Yet, if the individual characteristics matter when modeling the disease, the overall estimation of the epidemic evolution relies on a non-specified percentage of the global population : it is not based on the state of health of each individual. The goal of this paper is to propose a model that relies on a daily evolution of the individual's state, which depends on their mobility and the characteristics of the area they visit. Thus, the mobility data of a single person moving from one area to another, gathered thanks to mobile networks, is the essential building block to predict the disease outcome. We implement our solution and demonstrate its effectiveness through empirical experiments. The results show how promising the model is in providing possible insights into the failure of the disease control in the Kedougou region.

1 INTRODUCTION

Human malaria is caused by infection by the *Plasmodium falciparum* and four other species of parasites, leading to almost 600,000 deaths and 100–250M febrile episodes annually WHO Inc. (2016). Even though the disease has been investigated for hundreds of years, it still remains a major public health problem in Sub-Saharan Africa (SSA) where about 90% of malaria cases were reported in 2017 WHO Inc. (2016).

Many SSA countries have set the goal of eliminating malaria for the upcoming decades outbreaks Ruktanonchai et al. (2016). Among these countries, Senegal has initiated its National Program Against Malaria (PNLP) du Sénégal (2017). Besides a weekly follow-up of the disease evolution, the PNLN has allowed to intensify the coverage of key malaria interventions over the country in terms of impregnated mosquito nets, insecticide (ITN), indoor residual spraying, preventive treatment by intermittent administration to women intestines (TPI), rapid diagnostic tests (RDTs) and therapeutic combinations based on Artemisinin (CTA) Thiam et al. (2011). Those strategies have

lowered the malaria incidence (relative number of infected people for 1000 inhabitants) to a relative small number estimated to 25 in 2017. However, the south-eastern part of the country (Kedougou region alongside Kolda and Tambacounda) accounts for 75% of malaria cases and 45% of malaria-related deaths. Specially, the malaria incidence was estimated to 429 in 2017 for Kedougou while the other regions of Senegal had an average incidence below 10. Such situation on Kedougou reveals the weaknesses of the overall strategies taken to face the disease, and why malaria pre-elimination remains a crucial problem in the country. In this work, we investigate Kedougou case to show forgotten aspects in antimalarial policies and to demonstrate that more efficient actions should be considered.

Actually, Kedougou is the largest city in south-eastern Senegal 700 km away from Dakar which is the capital. Kedougou has a dry tropical climate, with an average annual rainfall over 1000 mm, spread over a rainy season that lasts from May to November. It is a mainly agricultural region with the cultivation of cereals (rice, corn, sorghum, millet, fonio ...) and many forest fruit species including mango, shea, palm, etc.



Figure 1: Kedougou region with its 3 departments.

Moreover, it offers a variety of natural attractions including those of the Niokolo Koba national park, the hills where trekking activities are practiced and the Dindéfelo waterfall. The discovery of deposits of uranium, granites, marble and other ornamental rocks, but also industrial minerals such as phosphate and kaolin ranks Kedougou as a cornerstone mining region. All these characteristics, along with its proximity to Mali and Guinea make Kedougou a true crossroads all over the year, which leads to a strong human mobility rate. As shown in the Figure 1, the region of Kedougou is divided into three departments, namely, Salemata with 14.6 % of the population, Kedougou department that shelters 51.9% and Saraya, 33.5% ANSD (2013). As depicted on the map, Kedougou department is on the center of the region and hosts the main infrastructures such as markets, health centers, and so on. This geo-administrative division raises an intra-mobility rate of individuals within Kedougou region.

As a conclusion, Kedougou region is characterized by two types of mobility : an intra-mobility for daily or weekly needs of permanent residents, and an extra mobility at the country and the west African community level. Our goal is to provide tools highlighting the negative incidence of these mobility patterns on the malaria disease.

Some statistical data from the PNLP and related to Kedougou region du Sénégal (2017) are used to plot the Figure 2, that shows the variation of new malaria cases over 24 months, *i.e.*, from January 2016 to December 2017. The first observation is that the number of cases raises drastically just after the beginning of the rainfall season (each year on June, months 6 and 18) and decreases with the end of the rainy annual period (on September, months 9 and 21). This situation is explained by the fact that mosquitoes population is growing faster during rainy seasons. Therefore, since weather conditions are similar over two successive years, we almost observe the same seasonal trend.

However, when looking deeper at the three curves, we find out that the epidemic of the three departments are not similar. First of all, the different peaks of

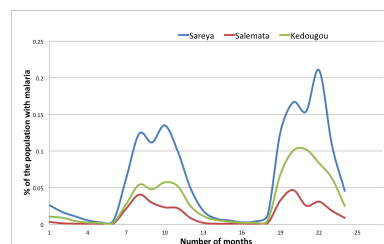


Figure 2: The Variation of malaria between Jan. 2016 and Dec. 2017.

the malaria cases in each departments do not occur at the same time and are actually staggered by a few weeks. Moreover, we note that the epidemic in Saraya lasts longer than the ones in Kedougou or Salemata even though the three departments have similar climatic conditions. Thus, rainfalls do not fully explain the spread of the epidemic over 6 months. Still, we know that there is a lot of movement towards the zone (trade and mining with other border countries). Also, it has been demonstrated that human mobility has an impact on malaria control and elimination Gharbi et al. (2013); Ruktanonchai et al. (2016) and even in malaria-free countries Dharmawardena et al. (2017). Bearing this in mind, it makes sense to relate the epidemic outbreak of a given area to the arrival of outsiders who have been exposed in other areas during different periods. Surprisingly, despite the strong sustained mobility around the Kedougou region, the PNLP does not include human movements in its control strategies yet.

We make the assumption that the arrival of infected people in a given area makes the epidemic to last longer. The impact on the epidemic extension depends on the arrival date of new people and the epidemic state of the area they come from. Our goal is to demonstrate that this assumption is plausible through a mathematical model. In fact, mathematical models have been frequently used in related works about malaria control Chitnis et al. (2006); Dimitrov and Meyers (2010); Mandal et al. (2011); Chitnis et al. (2008); Arthur (2017); Ruktanonchai et al. (2016); Greenwood et al. (1991); Gu et al. (2003a); Koella (1991); Filipe et al. (2007); Lechthaler et al. (2019). Existing models consider different parameters and aspects that influence the disease dispersal, such as heterogeneity, immunity, recovery time and more recently, human mobility. However, the models with human mobility only deal with the movement of people through a coarse grain approach, which assumes a global migration ratio from an area to another one. Rather, a finer grain approach can be used thanks to personalized geo-position information (GPS coordinates) from mobile phones. Such a finer approach al-

lows a better understanding of the disease evolution at each time, on each area. Therefore, it helps to determine the antimalarial actions in a more dynamic and efficient fashion.

The main contributions of this paper can be summarized as follow:

- We define a mathematical model that takes into account individual mobility and immunity. To this end, we assume that we have real-time data from mobile devices allowing to establish the mobility pattern of everyone, and his(her) state wrt. the malaria (ill or not). Hence, we build a discrete model that mainly differs from existing works by the fact that the global status of a given space is obtained by aggregating the health status of each individual.
- We implement a simulation software with respect to climatic conditions and human movements over time. The software is designed so that the relevant parameters of the disease can be adjusted according to the real life situation of a given area.
- We conduct a set of experiments to validate our approach while we point out many benefits of our solution in terms of explaining the disease evolution in areas like Kedougou. To this end, we rely on synthetic data according to realistic scenarios since real-time data are not available yet. We show the impact of different factors (characteristics of areas, mobility and state of individuals) on the malaria propagation. This allows for measuring the impact of malaria control actions (eradication, prevention) in an accurate way, which helps deciding which actions should be prioritized.

2 BACKGROUND

Mathematical models have been used to predict the occurrence of a disease and to control its dispersal. Basically, the modeling methodology is mainly deterministic and based on differential equations while selecting clinical and biological features that seem to be important Greenwood et al. (1991); Chitnis et al. (2006, 2008); Arthur (2017); Ruktanonchai et al. (2016). The first models that were developed examine the interaction of human, vectors and parasites with a coarse granularity, for instance, at the city/country level Mandal et al. (2011). More recent models have attempted to handle heterogeneity such as the individual immunity Gu et al. (2003a); Filipe et al. (2007), the space and contact network Parham and Ferguson (2006), the recovery rate Gu et al. (2003b), etc. A recent work integrates human mobility data Ruktanon-

chai et al. (2016) for explaining and eliminating the disease in a particular area.

One of the first model, known as the classical "Ross model", was developed by Sir Ronald Ross who explained the relationship between the number of mosquitoes and incidence of malaria in humans Ross (1911). In such a model, the population is divided into several *compartments* which represent health statuses regarding the pathogen. These statuses or compartments are represented by the standard notation *S-E-I-R*, based on the work presented in Kermack and McKendrick (1927). The *S* class stands for the fraction of host population that is susceptible to infection, while the *E* category indicates the fraction of population whose individuals have been infected but are not infectious yet due to a latency period. The *I* class represents infectious individuals who may infect other individuals through interactions with mosquitoes. Finally, the *R* class portrays individuals who have recovered from the infection. Notice that sometimes, *R* may include individuals who have recovered with temporary or permanent immunity. With these different classes, one may observe eight possible models: *SIS*, *SEI*, *SEIS*, *SIR*, *SIRS*, *SEIR* and *SEIRS*. Note that both mosquito and host population may be related with these compartments in a malaria disease case. That is, the malaria transmission model is described along two aspects, one representing humans and the other representing mosquitoes. However, a mosquito can not recover from being infected, so its infective period ends with its death.

3 DISCRETE MALARIA MODEL

As we pointed out earlier, we aim at integrating user mobility information into a malaria transmission model. The reason behind this is that knowing the mobility and state of each individuals allows for assessing the specific persons that diffuse the disease instead of finding a proportion of population as done by existing models. In this sense, our approach differs to others by the fact that we estimate the probability of each individual to be part of one class (SEIR), and therefore, we deduce the global population that belong to each class at each time unit.

3.1 Global Model Overview

We assume a multi-patches area where each patch has a specific configuration to impact the malaria disease propagation. Individuals can move from one patch to another while mosquitoes are set to stay in only one patch. To model the transmission, we extend the

SEIRS-SEI model proposed in Chitnis et al. (2008) by introducing patches and individuals data mobility. Fig. 3 shows the proposed malaria transmission model. Solid arrows denote intra-species progression into classes while dotted arrows denote inter-species transmission. With this model, for each patch i the

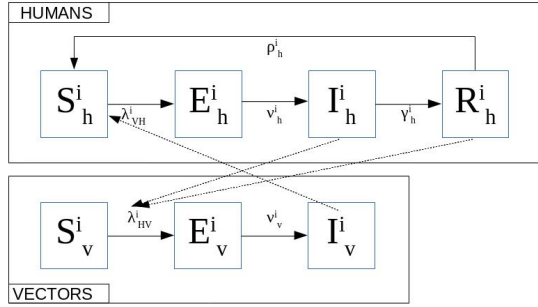


Figure 3: Malaria model in patch i Chitnis et al. (2008).

human population is divided into four classes: susceptible S_h^i , exposed E_h^i , infectious I_h^i , and recovered (partially and/or temporary immune) R_h^i . Moreover, mosquitoes population is divided into three classes: susceptible S_v^i , exposed E_v^i , infectious I_v^i . We assume a constant population (*i.e.*, birth rate equals death rate). Initially, all individuals are in the susceptible class except a low percentage that live with the parasites. This situation is realistic in a context where the malaria parasite is still present. Basically, a proportion of the susceptible individuals that move from the S to the E class due to mosquito bites is characterized by the *force of infection* (FoI) λ_{vh}^i . Among exposed individuals, there is a proportion v_h^i that enter to the infectious class. v_h^i depends on a time period, called an intrinsic incubation period, which depends on the parasite species (*i.e.*, *Plasmodium falciparum*). Later on (approximately a couple of weeks), a part of infectious humans (γ_h^i ratio) recover and join the R class where they may acquire a certain immunity to the disease and do not get clinically ill. However, they still host low amount of parasites and can transmit the infection to mosquitoes with a low rate. Over the time, the immunity of individuals vanishes and a some of them (ρ_h^i ratio) return to the S class. Regarding the mosquitoes population, the same flowchart is observed with only three classes. It is worth noting that the mosquitoes FoI (λ_{hv}^i) differs from humans' FoI, so does the incubation period of mosquitoes and humans. The main parameters of the model are divided into two categories: patch parameters and individual parameters. In the following, we present a short overview of these parameters.

3.2 Dealing with Patch and Individual Characteristics

3.2.1 Patch Characteristics

Since our model is discrete, we define the transmission in patches at a given time step t . For each patch i , we use almost the same parameters as described in Chitnis et al. (2008) while adapting them to a multi-patches context (see Table 1 for parameters details).

After identifying the required parameters, we define the vector-to-human FoI (λ_{vh}^i) and human-to-vector FoI (λ_{hv}^i) in a patch as follows :

$$\lambda_{vh}^i(t+1) = b_h^i(t) \beta_{vh}^i \frac{I_v^i(t)}{N_v^i(t)} \quad (1)$$

$$\lambda_{hv}^i(t+1) = b_v^i(t) (\beta_{hv}^i \frac{I_h^i(t)}{N_h^i(t)} + \tilde{\beta}_{hv}^i \frac{R_h^i(t)}{N_h^i(t)}) \quad (2)$$

3.2.2 Individual Mobility Characteristics

We distinguish residential patches (cities or districts) to *ad-hoc* meeting patches. Meeting patches (P_M) are sparsely populated and used as headquarter for social events while residential patches (P_R) are densely populated but not attractive for social meetings. Having this in mind, one may deduce that people more often move from P_R to P_M than from P_R to P_R . We assume that each individual is identified thanks to mobile applications and/or Telecommunication companies. Users data are anonymised in such a way that personal details are hidden while geographical positions of anonymous individuals are known at each time. We consider a sequence of consecutive time windows of equal duration. At anytime, the patch of an individual h_j and how long he stays there are known. For instance, on Figures 4a and 4b, human h_j stayed during w_j^1 time in p_1 , w_j^2 in p_2 , and so on.

For individual h_j , his probability of being exposed is a function of his status and FoI, which depends on his mobility as well as his immunity. Basically, the FoI of an individual is the sum of the FoI of each visited patch i weighted by its time presence in i :

$$\lambda_{h,j}(t) = \sum_{i=1}^N w_j^i(t) \lambda_{vh}^i(t) \quad (3)$$

Finally, the likelihood to get exposed of h_j at time $t+1$ is : $pe_j(t+1) = pe_j(t) + \lambda_{h,j}(t)(1 - pe_j(t))$. Once an individual is exposed, the incubation, development and recovery process are a matter of time. Basically, an exposed human has a likelihood to get infected and to recover after a certain period. Details of parameters

Table 1: Patches Parameters.

Parameter	Description
$N_h^i(t)$	Human population in patch i at time t
$N_v^i(t)$	Vector population in patch i at time t
$I_v^i(t)$	Infected mosquitoes in patch i at time t
$I_h^i(t)$	Infected humans in patch i at time t
$R_h^i(t)$	Infected individuals in patch i that recover at time t
β_{hv}^i	Probability that an infectious person infects a susceptible mosquito during a contact within the patch i
β_{vh}^i	Probability that an infectious mosquito infects a susceptible individual during a bite in patch i
$\tilde{\beta}_{hv}^i$	Probability that a recovered person infects a susceptible mosquito during a contact in patch i
$b_h^i(t)$	Proportion of bites per human per unit time t in patch i
$b_v^i(t)$	Proportion of bites per mosquito per unit time t in patch i
λ_{vh}^i	Force of infection from vector to human in patch i , <i>i.e.</i> , measure of how likely a human get exposed in patch i
λ_{hv}^i	Force of infection from human to vector in patch i , <i>i.e.</i> , measure of how likely a mosquito get exposed in patch i

Table 2: Individual Parameters for a given time window.

Parameter	Description
h_j	Identification of the individual j
w_j^k	Visiting ratio of time that h_j spends in patch k .
$S_{h,j}(t)$	Susceptible state variable of h_j at time step t (1 if susceptible 0 otherwise)
$E_{h,j}(t)$	Exposed state variable of h_j at time step t (1 if exposed 0 otherwise)
$I_{h,j}(t)$	Infected state variable of h_j at time step t (1 if infected 0 otherwise)
$R_{h,j}(t)$	Recovered state variable of h_j at time step t (1 if recovered 0 otherwise)
$pe_j(t)$	Probability that individual h_j (being in class S) moves to class E
$\nu_{h,j}$	incubation period (without symptoms). In the case of <i>P. falciparum</i> parasite, which predominates in Senegal, it varies from 9 to 10 days Chitnis et al. (2008); for Disease Control and Prevention (2015).
$\frac{1}{\gamma_{h,j}}$	is the infectious period (Chitnis and Al. have set it at 9.5 months Chitnis et al. (2008))

for calculating the transition over the classes SEIR are described in Table 2.

After defining FoI of individuals, we identify at each time the new exposed ones, and apply the model to get the class of the other individuals. With the above parameters, we aggregate individual information to get patch-level information. The human population over the different classes is defined for each patch and each time period, as follows :

$$S_h^i(t) = \sum_{j=1}^M w_j^i(t) S_{h,j}(t) \quad (4)$$

$$E_h^i(t) = \sum_{j=1}^M w_j^i(t) E_{h,j}(t) \quad (5)$$

$$I_h^i(t) = \sum_{j=1}^M w_j^i(t) I_{h,j}(t) \quad (6)$$

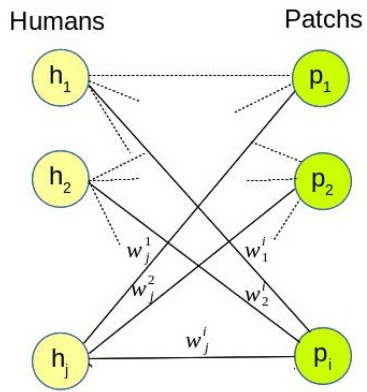
$$R_h^i(t) = \sum_{j=1}^M w_j^i(t) R_{h,j}(t) \quad (7)$$

The variation of mosquitoes population over the classes is the same as described in Chitnis et al. (2008) :

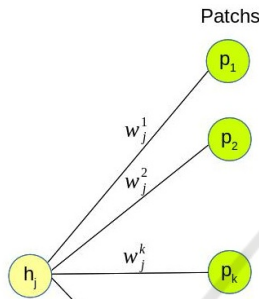
$$\frac{dS_v^i}{dt} = \Psi_v^i N_v^i - \lambda_{hv}^i(t) S_v^i - f_v^i(N_v^i) S_v^i \quad (8)$$

$$\frac{dI_v^i}{dt} = \nu_v^i E_v^i - f_v^i(N_v^i) I_v^i \quad (9)$$

$$\frac{dE_v^i}{dt} = \lambda_{hv}^i(t) S_v^i - \nu_v^i E_v^i - f_v^i(N_v^i) E_v^i \quad (10)$$



(a) Individuals visiting different patches
Human j



(b) Mobility pattern of an individual

Figure 4: Human mobility and Patches

where $f_v^i(N_v^i) = \mu_{1v}^i + \mu_{2v}^i N_v^i$ is the per capita density-dependent death rate for mosquitoes in the patch i Chitnis et al. (2006).

It is worth noting that our model is computed in an incremental way. After each time step, we update the information describing patches and individuals (*i.e.*, FoI and health status) since they are used as input for the next time step.

4 IMPLEMENTATION AND VALIDATION

4.1 Experimental Setup

We implemented our approach using the version 2.7.15 of Python through Spyder IDE 3.2.6 on Linux. We rely on Jupyter for visualization and share the

source code of our implementation¹. All the parameters about individuals and patches we used to implement the model are detailed in section 3.2. We recall that most of these parameters values have been reported in the literature.

We consider two patches : the residence zone P_R and the meeting one P_M , with their respective human population $|P_R|$ and $|P_M|$, their respective vector (mosquito) population NV_R and NV_M and the proportion p of human traveling from P_R to P_M . We observe I_R , the number of infected persons in P_R . Table 3 summarizes the parameters used in the experiments.

4.2 Experimental Objectives and Method

The overall goal of the validation is to investigate the benefit of individual mobility for malaria control. We intend to show that taking into account individual mobility allows for a more accurate modeling of the disease evolution over time and space (*i.e.*, patches). We aim to simulate disease evolution which cannot be captured by existing models that are unaware of individual mobility. Precisely, we evaluate the gain of our approach in three different aspects:

1. The impact of individual mobility on the estimation of infected individuals.
2. The relevance of the proposed model to approximately match recently reported real cases.
3. The vector control opportunities based on individuals movements and patches characteristics.

4.2.1 Size of the Vector Population over Seasons

In this section, we only consider the P_R patch, thus we omit the R indice in the notations. To be as close as possible to what happens in the real world, we vary the population of (mosquito) vectors according to the two main seasons occurring in the Kedougou region:

- the rainy season (approximately from start of June to the end of November)
- the dry season (the remaining 6 months).

The number of mosquitos grows *wrt.* a daily birth rate (ψ , see Section 3). This birth rate still grows and reaches a stationary value when the rainy season settles definitively. Indeed, the mosquito birth rate is correlated with the amount of wet place (reproduction areas). All potential wet places are full of water when the rainy season is in full swing. Thus, we assume that during the rainy season the total size of

¹www-bd.lip6.fr/wiki/site/recherche/projets/m4e/start

Table 3: Experimental parameters.

name	description	value
P_R	the residential patch	
$ P_R $	the number of individuals in P_R	3000
NV_R	the number of vectors in P_R	Varying
P_M	the meeting patch	
$ P_M $	the number of individuals in P_M	1000
NV_M	the number of vectors in P_M	Varying
p	the ratio of moving individuals ($p > 0$)	[0.1, 0.4]
I_R	the number of infected individuals in P_R	[0, 3000]
ψ	vector birth rate	0.03
μ	vector death rate	[0.03, 2E-8]

these wet areas remains almost constant therefore the vector population NV_{max} remains almost constant.

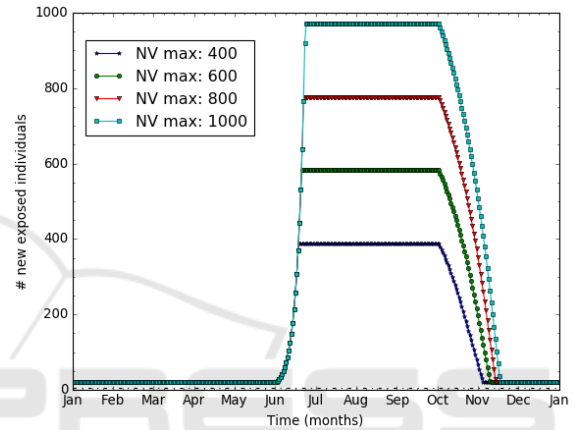
Then, at the end of the rainy season, the vector population is gradually decreasing up to the dry season ceiling (*i.e.*, a rather small number that makes the epidemic to stop itself). The death rate (μ see Table 3) is based on the average life duration of a vector (30 days).

Figure 5(a) plots the number of vectors over time during one year for the residential patch, with different characteristics in terms of wet areas. For instance, in the first case ($NV = 400$) the vector population is 20 times higher than during the dry season, whereas in the last one, ($NV = 1000$) it is 50 times higher. This allows for simulating areas with different characteristics in terms of wet areas and therefore in terms of vectors population growth. Note that these areas are located in the same region thus have **similar** rainy seasons (from June to November).

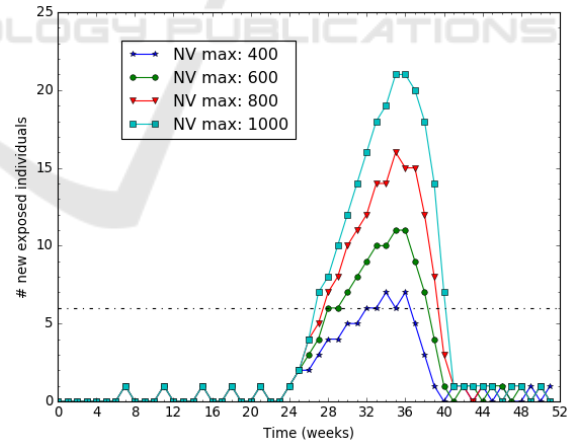
To figure out the effect of the rainy season on the disease, we compute the number of newly infected individuals in P_R patch when everyone remains sedentary (*i.e.*, no mobility). Figure 5(b) reports the results for the 4 patches from Figure 5(a). In the first patch ($NV = 400$) there is almost no disease while in the 3 other ones, the peak disease grows for patch having more vectors. We use these preliminary simulations, to set the maximal number of vectors (denoted NV_{max}) that a residential and meeting patch have in the subsequent experiments. This allows us to define a low endemicity residential patch ($NV_{max} = 400$) and a higher endemicity meeting patch ($NV_{max} = 1000$)

4.3 Impact of Individual Mobility

The goal of this section is to quantify the impact of individual mobility in modeling malaria. Based on the Kedougou case (*cf.* Section 1), we consider a village of farmers that sell their products at a remote market. Basically, there are two patches: a residential place P_R and a market place P_M . There are 3000 people living



(a) NV max varying from 400 to 1000.



(b) # new exposed indiv. vs. NV max.

Figure 5: Impact of the maximum number of vectors (NV_{max}) on the disease.

in P_R . Among them, a group of people (which size ratio is p relative to P_R population) moves everyday from P_R to P_M and come back home.

4.3.1 Varying the Mobility Rate

The goal of this experiment is to assess the impact of the mobility on the disease evolution. First, we define the *mobility rate* r as the ratio of people moving from P_R to P_M . Then we investigate how the number of exposed individuals, $E(r)$, evolves over time for various mobility rates. To this end we vary the mobility rate, r , from 0% to 40%. On Figure 6, we report the number of newly infected individuals per week.

The dashed black line indicates the threshold limit of exposed people. Above this threshold, the disease is qualified as an epidemic situation. The threshold value is set to 6 new cases per week according to real observations reported in Kedougou during years 2016 and 2017 du Sénégal (2017).

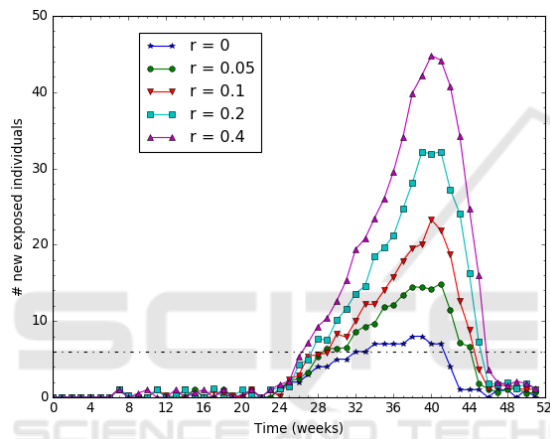


Figure 6: Varying the mobility rate r from 0 to 40%.

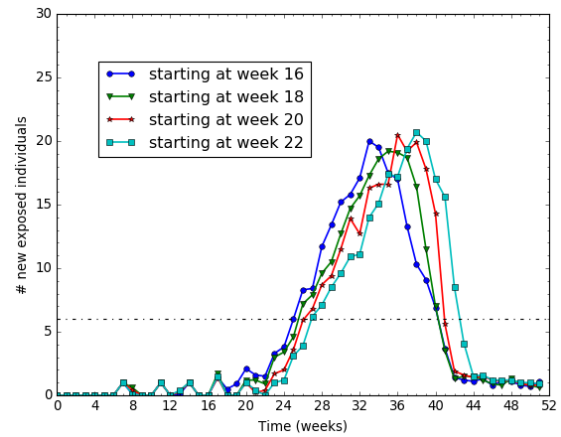
We observe on Figure 6 that the higher the moving rate, the higher the epidemic and longer is the epidemic duration too. For example, when nobody is moving ($r=0$), the epidemic lasts 8 weeks with 7 new cases per week; whereas for a moving rate of 10%, it lasts 16 weeks and reaches a peak of 25 cases per week.

4.3.2 Early/Late Rainy Season in the Meeting Patch P_M

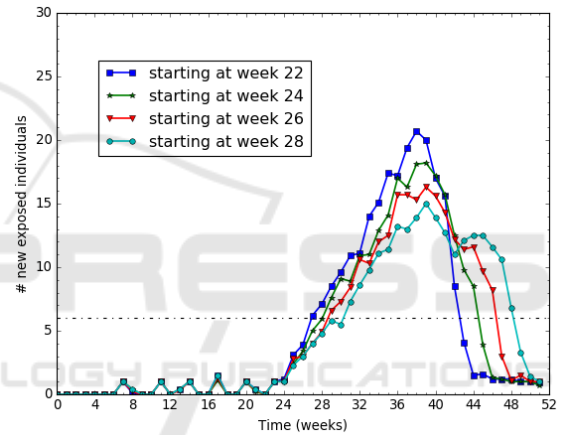
In case the mobility patch and the residential patch have slightly different raining seasons, this could have an impact on the epidemic duration.

In this section, we study the impact of having a rainy season in P_M that does not start exactly at the same time as in P_R . The rainy season in P_R lasts from week 22 to week 38 (*i.e.*, 16 weeks from June to September). The P_M rainy season lasts as long as the P_R one but it starts before or after week 22. The mobility pattern is set to 20 % mobile individuals that go to P_M every day for half of their time. We report on

Figure 7 the number of exposed individuals for several starting dates of the P_M rainy season.



(a) Starting in P_M earlier than in P_R .



(b) Starting in P_M later than in P_R .

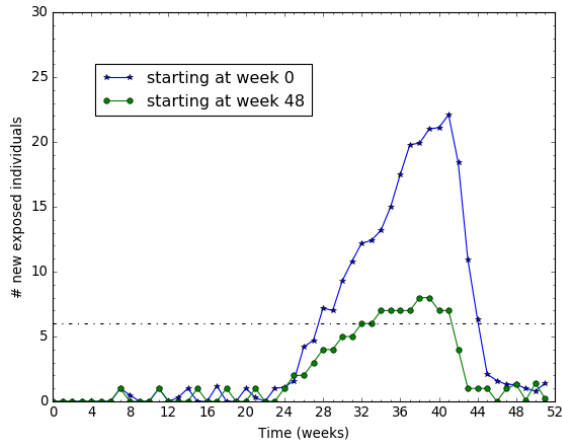
Figure 7: Varying the starting date of the rainy season in P_M .

The results show that the epidemic lasts longer on Figure 7(b) than on Figure 7(a). That is, it lasts longer when the rainy season starts in P_M later than in P_R . The extra time duration (between 2 and 6 weeks as reported in Figure 7(b)) of the epidemic corresponds to the rainy season starting time gap between the two patches.

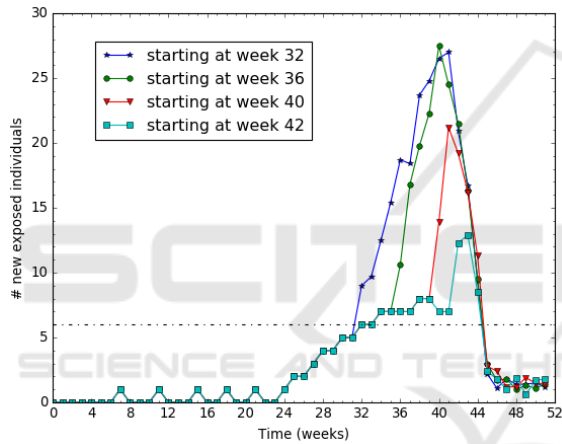
4.3.3 Varying the Mobility Starting Date

In this experiment, we vary the starting date (before this date, nobody moves) from $t=0$ (beginning of the year) to $t=40$ (late October). We want to investigate the impact of seasonal migration on the development of the disease. Intuitively, we expect a greater impact when the migration occurs during the rain season which has the highest vector population. Such migrations are usual in the Kedougou region, where there

are few fair places and people from small cities or villages have to move to sell or buy goods.



(a) Mobility starting before/after the rain season.



(b) Mobility starting during the rain season.

Figure 8: Impact of the mobility starting date on the disease.

With 20% moving people and other parameters set similar to the ones used in previous experiment (section 4.3.2), we plot on Figure 8 the impact of the starting mobility on the disease evolution.

The results (for "Week 40" curve) suggest that the disease development is quite slow before the migration start. When the migration starts at the beginning of the rain season (see "Week 0" curve), the disease grows slowly because most of the vectors are still in a susceptible state implying a low vector-to-human FoI. On the other hand, when a migration starts at the middle of the rain season (see "Week 32" and "Week 36" curves), the disease grows very fast because most of the vectors are already infected, thus, causing a high FOI.

Figure 9 aggregates 2 different cases of migration patterns occurring on 2 sub-areas: a migration starting

at week 0 and another one starting at week 40. We report (in red curve) the total number of newly exposed people on the area.

The results suggest that the disease lasts 35 weeks, which is longer than any of the two sub-areas. More interestingly, the disease lasts 8 weeks longer than the longest epidemic plotted on Figure 6. Notice that the two sub-areas do have the same rain season because they are located in the same region. We can conclude that successive migrations from various specific areas (close villages) tend to generate rather long epidemic at a higher scale (region level). The results are consistent with the real Kedougou observations : they provide a possible explanation of what happened at Kedougou.

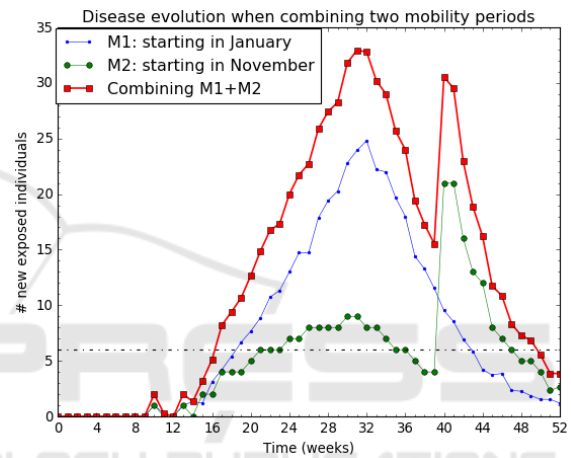


Figure 9: Aggregating on 2 zones.

4.4 Relevance of the Model to Match the Kedougou Real Case

The objective is to evaluate the relevance of our model to match real malaria observations recently reported in PNL (2017). An observation is reported as a series of newly infected people, one value per week. Given a observation occurring in an area of P inhabitants for a period of n weeks, we define a normalized report $R = \{R_1, \dots, R_n\}$ such that R_i is the number of newly infected people for week i divided by the population P . Let M be a model for the observation reported by R . Running M generates $\{M_1, \dots, M_n\}$ such that M_i is the expected ratio of newly infected people on week i .

We plot the obtained values in Figure 10 and the relative accuracy is $E_{M,R} = 0.016$, what gives a mean absolute error $MAE = 0.001$. These results show that the values measured (reports) and those calculated with the model differ by approximately 1 case per 1000. Therefore we can say that our model produces

values that are close to what is reported from real observations.

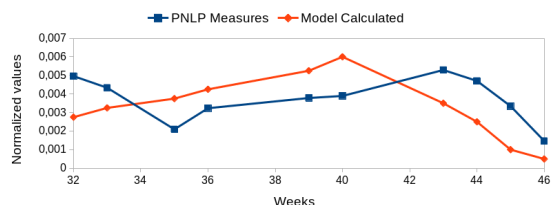


Figure 10: Normalized values from real observations vs. simulation.

Therefore, using our model can help for more efficient malaria control actions. For example, using the model one can decide on which location to conduct preventive actions in priority.

4.5 Vector Control Efficiency

In this experiment, we measure the benefit of our approach on controlling the malaria vectors. There are two types of malaria control actions: 1) a *preventive action*, which consists of convincing people to use repellent and mosquito nets in order to avoid mosquito bites, and 2) an *eradication action* (i.e., mosquito removal) that consists in suppressing most of the vectors in an area using chemical products. Notice that this second action type may have dramatic ecological consequences. Therefore, the first action type, preventive, would be a better choice. However, it comes at a cost that must be optimized.

We aim to show that preventive action helps reducing the vector-to-human FoI and then reduce the epidemic intensity and duration.

We already show in previous sections, that the moving part of the population is the major factor that impact the epidemic duration and intensity. We now protect those people who move from residential patch to meeting patch. Actually, this protection could be done through repellent and mosquito nets. In this respect, we consider the experiment configuration where individuals mobility rate is 10% (see figure 6 when $r = 0.1$) and we use different values of protection rate (ptr) for people who regularly move. The protection rate ptr depicts the ratio of protected people among the moving ones. The results of these experiments are shown on Figure 11.

We show that for $ptr = 1$ when we protect 100% of the moving population, the epidemic intensity and duration is as low as if no people is moving (see the $r = 0$ case in figure 6). Therefore, preventive actions targeting moving people can be rather efficient. In a residential patch where few people are moving, such preventive action would be cost-optimized assuming

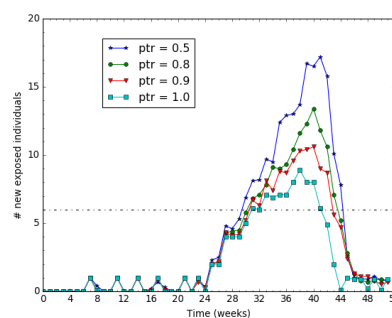


Figure 11: Malaria evolution according to the mosquito control strategy.

that the preventive action cost per individual is low. When p is varying from 1 to 0.8, the total number of exposed individuals is growing respectively from 118 to 169. This means that the preventive action must be rather complete to be efficient.

5 DISCUSSION

Among the various outcomes of the model, one may retain the following ones.

- **Risk Customizing.** The model helps to compute the likelihood p_E of a given individual to get exposed based on its mobility pattern through the different patches over the time. We have shown how important it is to distinguish, within a patch, moving people from residential ones. In a context like Kedougou, such a fine-grained model advocates that truckers, traders, and others with a high mobility rate should be observed more carefully since their risk to get infected, with the disease dispersal knock-on effect, is more significant.
- **Reducing Antimalarial Costs.** Since the model is devised for each individual, it allows to target specific persons at higher risk than the overall population. Bearing this in mind and the fact that each antimalarial action costs, then using the model can contribute to reduce the necessary means for the surveillance, and eventually, the elimination of the disease. Moreover, with the tight budgets in developing countries, combined with the rapid growth of the demography as well as the explosion of other infectious diseases that create new priorities for governments, the proposed approach seems to come up at the right time for facing definitively against malaria.
- **Mobility Impact.** As shown in the validation section, mobility may have either a great or low impact on a visited patches. Therefore, the time-based follow-up of a patch FoI using individu-

als' mobility should go along with more clinical testings to reach better predictions. In opposite of current strategies applied in Kedougou, which do not include human mobility details and figure out the overall disease trends weeks or months later, our model instantly plots detailed information about malaria dispersal. Hence, policy makers may foresee the right actions to do in each patch even though the disease has not happened yet.

- **What-if Analysis Boost.** Last but not the least, our solution can be used to calibrate the overall actions against malaria. In fact, we can model the disease spread while asking or supposing a specific pattern. For instance, we can suppose (or eventually suggest) that people have to stay home during their incubation period in order to reduce the global evolution of the disease. Likewise, we can suggest them following a specific mobility pattern based on the FoI of different patches. In other words, we offer policy maker a tool that can be used as dashboard to evaluate different scenario and their effects.

Even if the experimental results we got are interesting and rather intuitive sometime, they could be more accurate with real mobility data. In ongoing work, we plan to acquire those data and conduct deeper experimental validation.

6 CONCLUSION

In this article we proposed a malaria model that takes into account individual information such as mobility patterns, health statuses, and so on. The model is a discrete SEIR-SIS approach and differs mainly from existing models by the fact that global details about the disease are obtained by gathering the health status of each individual among a given population. Our approach is more accurate in terms of estimating the disease level, and affords the possibility to setup more efficient vector control strategies aiming to eliminate malaria in Africa. Actually, our model is an early explanation of Kedougou case where the malaria incidence is still high despite the strategies of the Senegal national program. In this respect, it unveils kind of solutions that decision makers can use with respect to individuals movement in order to eliminate the disease. Moreover, the results from our model match real observations in Kedougou with a mean absolute error of 0.001 while using synthetic data. Such a result is promising and let us believe that with real data, our approach will behave efficiently. Thus, ongoing works are conducted to collect on-line mobility data

obtained, for instance, through mobile networks. We are aware that the results presented in this paper are mainly based on synthetic data and thus cannot be interpreted as realistic results. However, as we obtain expected values we believe that our model behaves correctly and should give useful information when applied to real data in the future.

REFERENCES

- ANSD (2013). Projection de la population de la région de kedougou - 2013-2025. <http://www.ansd.sn/ressources/publications/indicateurs/Projections-demographiques-2013-2025+.htm>. Accessed: 2019-05-02.
- Arthur, S. (2017). Malaria incubation period. <http://malaria.emedtv.com/malaria/malaria-incubation-period.html>. Accessed: 2017-03-29.
- Chitnis, N., Cushing, J., and Hyman, J. (2006). Bifurcation analysis of a mathematical model for malaria transmission. *SIAM Journal on Applied Mathematics*, 67(1):24–45.
- Chitnis, N., Hyman, J. M., and Cushing, J. M. (2008). Determining Important Parameters in the Spread of Malaria Through the Sensitivity Analysis of a Mathematical Model. *Bulletin of Mathematical Biology*, 70(5):1272–1296.
- Dharmawardena, P., Rodrigo, C., Mendis, K., de A. W. Gunasekera, W. M. K. T., Premaratne, R., Ringwald, P., and Fernando, D. (2017). Response of imported malaria patients to antimalarial medicines in sri lanka following malaria elimination. *PLOS ONE*, 12(11):1–14.
- Dimitrov, N. B. and Meyers, L. A. (2010). *Mathematical Approaches to Infectious Disease Prediction and Control*, chapter Chapter 1, pages 1–25. INFORMS.
- du Sénégal, G. (2017). National malaria control program. <http://www.pnlp.sn/>. Accessed: 2019-01-25.
- Filipe, J. A., Riley, E. M., Drakeley, C. J., Sutherland, C. J., and Ghani, A. C. (2007). Determination of the processes driving the acquisition of immunity to malaria using a mathematical transmission model. *PLoS computational biology*, 3(12):1–11.
- for Disease Control, C. and Prevention (2015). <https://www.cdc.gov/malaria/about/disease.html>. Accessed: 2017-05-29.
- Gharbi, M., Flegg, J. A., Pradines, B., Berenger, A., Ndiaye, M., Djimdé, A. A., Roper, C., Hubert, V., Kendjo, E., Venkatesan, M., Brasseur, P., Gaye, O., Offianan, A. T., Penali, L., Le Bras, J., Guérin, P. J., and Study, M. o. t. F. N. R. C. f. I. M. (2013). Surveillance of travellers: An additional tool for tracking antimalarial drug resistance in endemic countries. *PLOS ONE*, 8(10):1–11.
- Greenwood, B., Marsh, K., and Snow, R. (1991). Why do some african children develop severe malaria? *Parasitology today*, 7(10):277–281.

- Gu, W., Killeen, G. F., Mbogo, C. M., Regens, J. L., Githure, J. I., and Beier, J. C. (2003a). An individual-based model of plasmodium falciparum malaria transmission on the coast of kenya. *Transactions of The Royal Society of Tropical Medicine and Hygiene*, 97(1):43–50.
- Gu, W., Mbogo, C. M., Githure, J. I., Regens, J. L., Killeen, G. F., Swalm, C. M., Yan, G., and Beier, J. C. (2003b). Low recovery rates stabilize malaria endemicity in areas of low transmission in coastal kenya. *Acta Tropica*, 86(1):71 – 81.
- Kermack, W. O. and McKendrick, A. G. (1927). A contribution to the mathematical theory of epidemics. *Proceedings of the royal society of london. Series A, Containing papers of a mathematical and physical character*, 115(772):700–721.
- Koella, J. C. (1991). On the use of mathematical models of malaria transmission. *Acta tropica*, 49(1):1–25.
- Lechthaler, F., Matthys, B., Lechthaler-Felber, G., Likwela, J. L., Mavoko, H. M., Rika, J. M., Mutombo, M. M., Ruckstuhl, L., Barczyk, J., Shargie, E., Prytherch, H., and Lengeler, C. (2019). Trends in reported malaria cases and the effects of malaria control in the democratic republic of the congo. *PLOS ONE*, 14(7):1–20.
- Mandal, S., Sarkar, R. R., and Sinha, S. (2011). Mathematical models of malaria - a review. *Malaria Journal*, 10(1):1–19.
- Parham, P. and Ferguson, N. (2006). Space and contact networks: capturing the locality of disease transmission. *Journal of the Royal Society Interface*, 3:483–493.
- PNLP (2017). Bulletin de surveillance sentinelle du paludisme. <http://www.pnlp.sn/bulletin-de-surveillance-sentinelle-du-paludisme/>. Accessed: 2019-08-30.
- Ross, R. (1911). *The Prevention of Malaria*. John Murray, Albemarle Street.
- Ruktanonchai, N. W., DeLeenheer, P., Tatem, A. J., Alegana, V. A., Caughlin, T. T., zu Erbach-Schoenberg, E., Lourenço, C., Ruktanonchai, C. W., and Smith, D. L. (2016). Identifying malaria transmission foci for elimination using human mobility data. *PLOS Computational Biology*, 12(4):1–19.
- Thiam, S., Thior, M., Faye, B., Ndiop, M., Diouf, M. L., Diouf, M. B., Diallo, I., Fall, F. B., Ndiaye, J. L., Albertini, A., Lee, E., Jorgensen, P., Gaye, O., and Bell, D. (2011). Major reduction in anti-malarial drug consumption in senegal after nation-wide introduction of malaria rapid diagnostic tests. *PLOS ONE*, 6(4):1–7.
- WHO Inc. (2016). OMS | 10 faits sur le paludisme. <http://www.who.int/features/factfiles/malaria/fr/>. Accessed: 2017-05-15.